Optimal Two-Impulse Rendezvous Between Two Circular Orbits Using Multiple-Revolution Lambert's Solutions

Haijun Shen and Panagiotis Tsiotras
Georgia Institute of Technology
Atlanta, GA 30332-0150, USA

AAS/AIAA Astrodynamics Specialist Conference
August 16–18, 1999

Optimal Two-Impulse Rendezvous Between Two Circular Orbits Using Multiple-Revolution Lambert's Solutions

Haijun Shen* and Panagiotis Tsiotras†
Georgia Institute of Technology
Atlanta, GA 30332-0150, USA

In this paper, we study the optimal fixed-time, two-impulse rendezvous between two spacecraft orbiting along two coplanar circular orbits in the same direction. The fixed-time two-impulse transfer problem between two fixed points on two circular orbits, called a fixed-time fixed-endpoint transfer problem, is solved first. Our solution scheme involves first the solution to the related multiple-revolution Lambert problem. A solution procedure is proposed to reduce the calculation of an existing algorithm, thanks to the introduction of an auxiliary transfer problem. Unlike the fixed-endpoint transfer problem with a fixed time of flight, the auxiliary transfer problem studies the relationship between the transfer cost and the transfer orbit semimajor axis with the transfer time being free. The characteristics of the auxiliary problem are thoroughly explored and then applied to the fixed-time fixed-endpoint problem. As a result, the solution candidates are narrowed down from $2N_{\max}+1$ ($N_{\max}$ is the maximum number of revolutions permitted) to at most two. Using this solution procedure, the minimum cost of the fixed-time transfer problem is easily obtained for all cases of different separation angles and times of flight. Thus a contour plot of the cost is obtained as a function of the separation angle and the transfer time. This contour plot along with a sliding rule facilitates the task of finding the optimal initial and terminal coasting periods, and thus obtaining the solutions for the original problem. Numerical examples demonstrate the application of the methodology to multiple rendezvous of satellite constellations on circular orbits.

Introduction

Orbital transfer problems using impulses have for a long time been part of the mainstream in space research. This can be very well justified by the large amount of references and several survey papers.[1–4] The majority of the earlier works (prior to 1960s) studied orbital transfers with free transfer time. More recently, and especially since the advent of Lawden's primer vector theory,[5] attention has been paid primarily on fixed-time orbital transfer problems.

In a cornerstone paper,[6] Lion and Handelsman applied calculus of variations to the primer vector and obtained the first order necessary conditions for adding an additional impulse to the trajectory, for finding the location of an interior impulse, and for adding initial and final coastings. A similar methodology was employed by Jezewski and Rozendaal[7] where they proposed a numerical procedure for obtaining optimal multiple-impulse solutions to orbital transfer problems. This procedure was later used by several authors to obtain optimal multiple-impulse solutions to specific problems in an ad hoc manner. Gross and Prussing[8] solved an optimal direct ascent time-fixed rendezvous problem. Two- and three-impulse rendezvous trajectories connecting an initial point at the planet's surface to a target in a circular orbit were sought. A variety of cases were investigated. For different initial relative locations of the chaser and target vehicles, and for different travel times, the regions where two- and three-impulse solutions are optimal, along with their corresponding costs, were determined. Prussing and Chiu[9] employed the same strategy to calculate the optimal multiple-impulse time-fixed rendezvous between two vehicles in circular orbits. Solutions with up to four impulses were obtained. Costs were plotted and compared for a variety of boundary conditions. In addition, the rendezvous problem between two inclined circular orbits was studied, albeit for a restricted case; namely, the chaser was assumed to be on the line of nodes at the initial time. Again, the costs and the optimal number of impulses were computed and were compared for a number of different boundary conditions.

Although for some rendezvous problems, multiple-impulse solutions use less fuel than two-impulse solutions, they suffer from the drawback of requiring a large number of computations. In fact, allowing more than two impulses offers only a limited benefit in terms of fuel expenditure. Most of the existing algorithms for multiple-impulse rendezvous follow the approach developed by Jezewski and Rozendaal.[7] Therein, the authors used nonlinear programming to obtain the optimal solutions. The convergence of the algorithms, however, is not guaranteed, and there are cases where the solutions converge to local minima. In addition, from an operational point of view, more impulses means increased hardware complexity and an increased possibility of failure. Therefore, in this paper we restrict

*Ph.D. candidate, School of Aerospace Engineering, Georgia Institute of Technology. Email: haijun_shen@ae.gatech.edu. Student member AIAA.

†Associate Professor, School of Aerospace Engineering, Georgia Institute of Technology. Tel: (404) 894-9526, Fax: (404) 894-2760, Email: p.tsiotras@ae.gatech.edu. Associate Fellow AIAA.

to two-impulse rendezvous only.

In this paper, we are interested in finding the best two-impulse solutions for a class of rendezvous problems. Specifically, we study the fixed-time two-impulse rendezvous problem between two spacecraft. Both the chaser and the target spacecraft move on two coplanar circular orbits in the same direction. The motivation for investigating such two-impulse fixed-time rendezvous problems stems from our interest in solving multiple rendezvous problems between several vehicles in a satellite constellation. Clusters of satellites and satellite constellations (including formation flying schemes) promise to provide increased flexibility, autonomy, reliability and operability compared to traditional single-spacecraft approaches.[10–12] In many cases, the satellites in the constellation can be serviced either from a vehicle launched from earth for that purpose or by other satellites in the same constellation.[13,14] Before being able to solve the multiple-rendezvous problem for a satellite constellation (which may include dozens or hundreds of satellites) it is imperative to have a complete characterization for the simplest case of an optimal rendezvous namely, between two satellites in a circular orbit. As a matter of fact, as shown in this paper, even the simple case of prioritizing the rendezvous maneuvers between three satellites is not clear from the outset. The results of this paper thus lay the foundation for solving efficiently optimal and suboptimal rendezvous strategies in a constellation of many satellites.

Apart from the aforementioned applications on satellite constellations on circular orbits, our work has also been motivated by a recent paper by Prussing[15] which studies the two-impulse multiple revolution Lambert problem. Since the two-impulse solutions may not be optimal in some cases, Lawden's primer vector theory cannot be used to obtain the solutions. Thus different approaches have to be undertaken. In Ref. 15 a solution procedure is outlined for a multiple-revolution Lambert problem. It is shown that given two points and a specified time of flight, if the time is long enough to allow $N_{\max}$ revolutions around the central body, there exist $2N_{\max}+1$ Keplerian orbits that pass through the given two points. Using the solutions to the multiple-revolution Lambert problem, Pussing[15] studies the minimum cost fixed-time transfer between two fixed points on coplanar circular orbits. He shows that allowing more than one revolution may reduce the fuel consumption. However, Ref. 15 does not identify which of the $2N_{\max}+1$ solutions renders the least cost. As a result, the minimum cost solution is obtained after calculating all $2N_{\max}+1$ candidates. In this paper, we provide an algorithm that quickly and efficiently identifies the optimal (minimum fuel) solution without the need to calculate all $2N_{\max}+1$ transfer orbits.

The paper is organized in the following manner. After the introduction, the formulation of the fixed-endpoint orbital transfer problem is presented, and an auxiliary transfer problem is introduced and analyzed. The solutions to the auxiliary problem are then applied to the fixed-endpoint transfer problem, and a solution procedure is suggested. The optimal two-impulse solution is then obtained by applying a sliding rule. As an application of this methodology, in the last section of the paper we analyze rendezvous maneuvers motivated by the problem of servicing satellites in a circular constellation.

Fixed-Time, Fixed-Endpoint Transfer Between Circular Orbits

Given two points in space P_1 and P_2, there are two elliptic orbits with the same semimajor axes that connect the two points, as shown in Fig. 1. In the figure F and F^* are

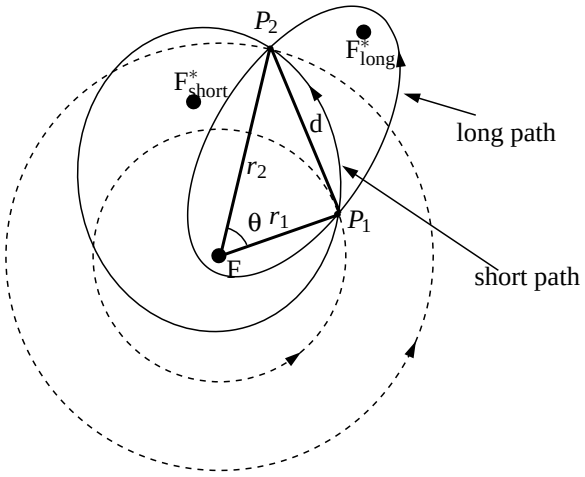

Fig. 1 Orbital geometry for Lambert problem.

the primary and secondary foci of the transfer orbits, r_1 and r_2 are the radii from F to the points P_1 and P_2 respectively, d is the length of the chord connecting P_1 and P_2, and θ is the central angle between r_1 and r_2. The two orbits in Fig. 1 belong to two categories, long path transfer orbit and short path transfer orbit. As seen in Fig. 1, for a long path transfer orbit, F and F^* lie on different sides of the P_1P_2 line segment, whereas for a short path transfer orbit, F and F^* lie on the same side of the P_1P_2 line segment. For a given transfer time t_f, an N-revolution transfer orbit stands for an elliptic orbit that passes through P_1 and P_2, and the time of travel along the P_1P_2 arc plus N complete revolutions is t_f. In general, there are more than one elliptic orbits that pass through P_1 and P_2 for a given travel time t_f, depending on the number of revolutions allowed. These orbits are long path and short path orbits with different semimajor axes.

According to Lambert,[16] the time of flight is only a function of the semimajor axis a, the sum of the radii r_1+r_2, and the chord d. Lagrange's formulation of the Lambert problem can be generalized to the multiple-revolution case as[15]

$$\sqrt{\mu}\,t_f = a^{3/2}[2N\pi+\alpha-\beta-(\sin\alpha-\sin\beta)] \qquad (1)$$

where μ is the gravitational parameter, N is the number of allowed revolutions, and α and β are defined as follows

$$\sin\frac{\alpha}{2}=\left(\frac{s}{2a}\right)^{1/2},\qquad \sin\frac{\beta}{2}=\left(\frac{s-d}{2a}\right)^{1/2},\qquad (2)$$

where $s=(r_1+r_2+d)/2$. A geometric interpretation of the variables α and β can be found in Ref. 17.

In the following, canonical units are used in the calculations. That is, the reference circular orbit has radius $r_1=1$ and period 1. Hence $\mu=4\pi^2$, and the velocity unit is the reference orbital speed divided by 2π.

An example plot of t_f vs. the semimajor axis a is shown in Fig. 2, based on Eq. (1). This plot corresponds to the case where $r_1=1$, $r_2=2$, and $\theta=60^\circ$. On the figure, the number of revolutions, N, is indicated. For each N, two solution branches exist, an upper branch and a lower branch. The upper branch corresponds to the long path for $\theta\le 180^\circ$, and the short path for $\theta\ge 180^\circ$; the lower branch corresponds to the short path for $\theta\le 180^\circ$, and the long path for $\theta\ge 180^\circ$. For each $N\ge 1$ there are two semimajor axes corresponding to one t_f, defining two N-revolution transfer orbits (short path and long path). For $N=0$ the lower branch is monotonically decreasing, so there is only one semimajor axis corresponding to one t_f (either short path or long path). Therefore, for a given t_f, there are $2N_{\max}+1$ solutions for the multi-revolution Lambert problem, where $N_{\max}$ is the maximum number of allowed revolutions. For example, in Fig. 2, it is shown that $N_{\max}=5$ for a time of flight of $t_f=7.6$, and it is clear that there is a total of eleven semimajor axes which determine eleven different transfer orbits connecting P_1 and P_2.

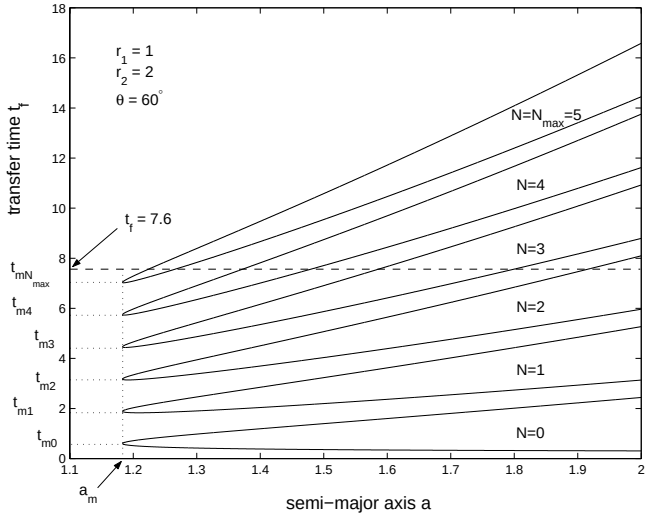

Fig. 2 An example graph of t_f vs. a.

It is well known that there exists a minimum-energy Keplerian orbit that connects two given fixed points in space.[16] The semimajor axis of this minimum energy orbit is given by $a_m=s/2$ which is the minimum semimajor axis as shown in Fig. 2 (same for all branches). The travel times corresponding to the transfer orbit with semimajor axis a_m and N revolutions are labelled as $t_{m\ell},\ \ell=0,1,\ldots,N_{\max}$. In Ref. 15, a procedure for determining $N_{\max}$ and solving for all the $2N_{\max}+1$ transfer orbits for a given t_f is given.

Although the Lambert problem is defined on two fixed points in space, regardless what the initial and terminal orbits are, in the following, we will consider minimum fuel, fixed-time, two-impulse transfer problems where both endpoints are in two unidirectional coplanar circular orbits, as shown in Fig. 1. For ease of reference we henceforth refer to this problem as the *fixed-time fixed-endpoint transfer problem*. Prussing[15] has listed and compared the minimum costs for various cases of ratios of orbital radii and central angles. He is interested in the question whether the long path or the short path transfer orbit renders the minimum cost. He also studies the optimal number of revolutions corresponding to the minimum cost solution. In Ref. 15 it is shown that there are no clear patterns facilitating the answers to these two questions. Therefore, a minimum cost transfer orbit is determined after all the $2N_{\max}+1$ solutions have been calculated and compared.

In the following sections, an *auxiliary orbital transfer problem* is introduced. This problem is slightly different than the formulation of the fixed-time fixed-endpoint transfer problem in the sense that the transfer time in the auxiliary transfer problem is free. It will be shown in the sequel that the solution to this auxiliary problem greatly facilitates the solution to the underlying fixed-time fixed-endpoint transfer problem. Indeed, at most two (instead of all $2N_{\max}+1$) solutions need to be calculated to yield the minimum cost.

The Auxiliary Transfer Problem

The auxiliary transfer problem also seeks the two-impulse minimum cost transfer between any two points P_1 and P_2 in two circular orbits. However, unlike the fixed-time fixed-endpoint transfer problem, in the auxiliary problem the time of flight is free. An explicit expression of the cost (the amount of velocity changes) needed to go from P_1 to P_2 along a Keplerian orbit can be obtained from classical orbital mechanics, as follows[18]

$$\Delta V=\Delta V_1+\Delta V_2 \qquad (3)$$

where ΔV_1 and ΔV_2 are the costs incurred at points P_1 and P_2. They are given by

$$\Delta V_i=\sqrt{v_i^2+v_{ic}^2-2v_iv_{ic}\cos\phi_i},\qquad i=1,2 \qquad (4)$$

where v_1 and v_2 are the orbital speeds at points P_1 and P_2 on the transfer orbit, v_{1c} and v_{2c} are the orbital speeds on the initial and terminal circular orbits, and ϕ_1 and ϕ_2 are the elevation angles, i.e., the angles at P_1 and P_2 between the velocities on the circular orbits and the velocities on the transfer orbit.

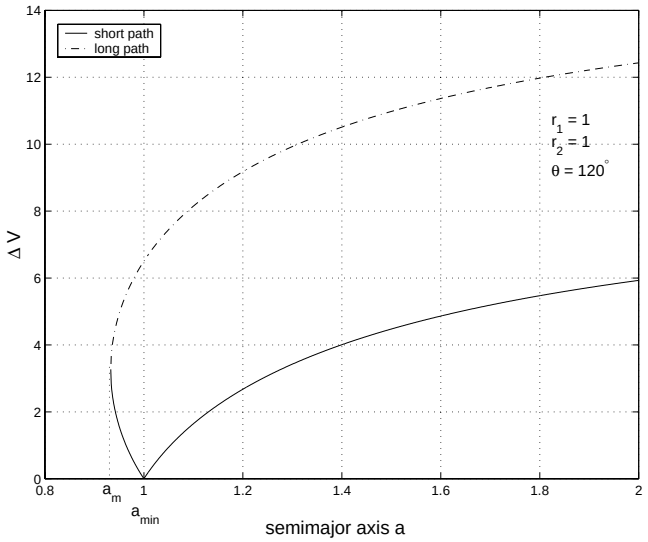

Fig. 3 ΔV **vs.** a**.**

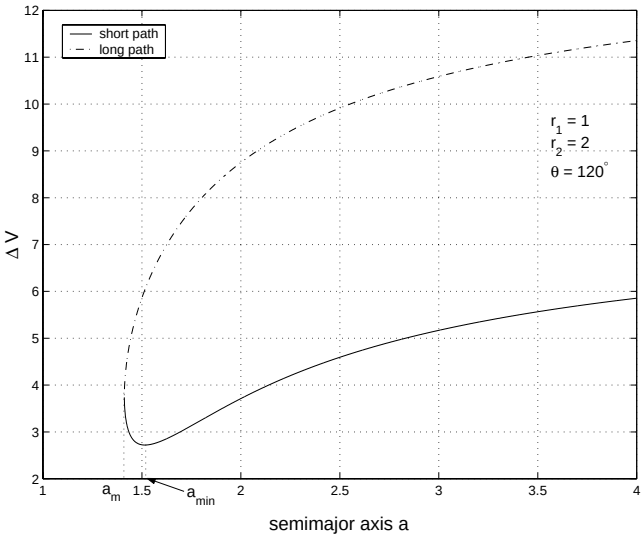

Fig. 4 ΔV **vs.** a**.**

It is worth noting that allowing for multiple-revolutions along a particular transfer orbit does not change the ΔV. However, the more revolutions are allowed, the longer the transfer time will be. As a result, as shown in Fig. 2 there are two transfer orbits passing through P_1 and P_2 which have the same semimajor axis. One is the long path transfer orbit, and the other the short path transfer orbit. These two transfer orbits correspond to different times of travel. It can be shown from fundamental orbital mechanics (see the Appendix) that the cost ΔV of the long path solution or the short path solution of the auxiliary orbital transfer problem is only a function of the semimajor axis of the transfer orbit. However, the analytical relationship between a and ΔV is rather complicated, as shown in the Appendix. Nevertheless, numerical results suggest a great deal of insight. Two plots of ΔV vs. a are shown here. The case where $r_1 = r_2$ is shown in Fig. 3, and the case where $r_2 = 2r_1$ is shown in Fig. 4. In both cases $\theta = 120^\circ$. It is worth pointing out that the plots for the two cases with central angles θ and $360^\circ - \theta$ are the same because of the symmetry of the transfer orbit.

Extensive numerical studies show that the ΔV vs. a plots for other combinations of r_1, r_2 and θ have similar characteristics as in Figs. 3 and 4. From these figures it is evident that there is a Keplerian transfer orbit that yields the minimum cost. The semimajor axis associated with this orbit is denoted by $a_{\min}$. This Keplerian orbit is the solution to the auxiliary transfer problem. Interestingly, this Keplerian orbit is always a short path transfer orbit. For the case where $r_1 = r_2$, it is intuitive that $a_{\min} = r_1 = r_2$, and that the total $\Delta V = 0$. Figure 3 shows that $a_{\min}$ is not a stationary point for ΔV. This can also be verified by referring to the Appendix where it is seen that $d(\Delta V)/da$ does not exist at $a_{\min} = r_1 = r_2$ because the eccentricity $e = 0$. However, for the case $r_1 \neq r_2$, Fig. 4 shows that $a_{\min}$ is a stationary point for ΔV. Hence $a_{\min}$ can be calculated by setting $d(\Delta V)/da = 0$ where ΔV is given in the explicit expression developed earlier. The detailed expressions for ΔV and $d(\Delta V)/da$ can be found in the Appendix.

As shown in Figs. 3 and 4, for a specific semimajor axis, following the long path transfer orbit is always more costly than following the short path transfer orbit. The cost associated with following a long path transfer orbit is monotonically increasing with a. Following the short path transfer orbit, however, the cost increases if the semimajor axis a is greater than $a_{\min}$, and is decreasing if the semimajor axis is less than $a_{\min}$. Caution has to be exercised because it is not true that any long path orbit always incurs larger cost than any short path orbit. For example, a short path transfer orbit with a large semimajor axis could be more costly than a long path transfer orbit with a smaller semimajor axis, as seen in Fig. 4.

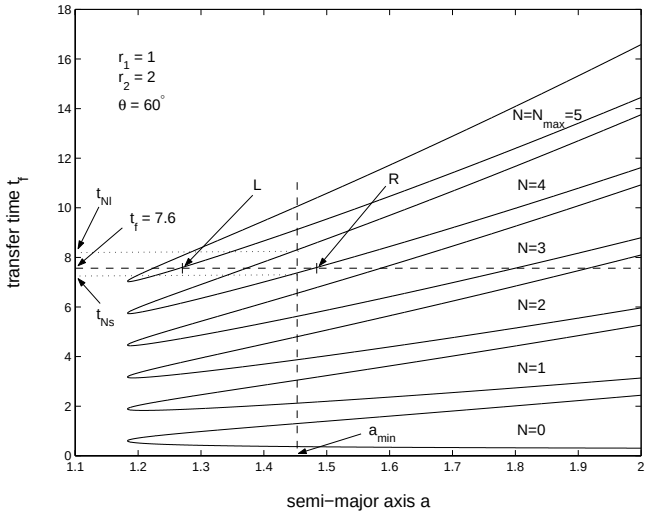

Fig. 5 Case 2.

Solution of the Fixed-Time Fixed-Endpoint Transfer Problem

Based on the observations made earlier about the characteristics of ΔV with respect to a for the auxiliary transfer problem, the computations required for the minimum cost solution for a fixed-time fixed-endpoint transfer problem can be significantly reduced. This is especially true for cases with large times of travel which may require a large number of revolutions. As a result, in some cases, the minimum ΔV solution is readily chosen, and in other cases, only two of the $2N_{\max}+1$ solutions need to be calculated and compared to obtain the minimum ΔV solution.

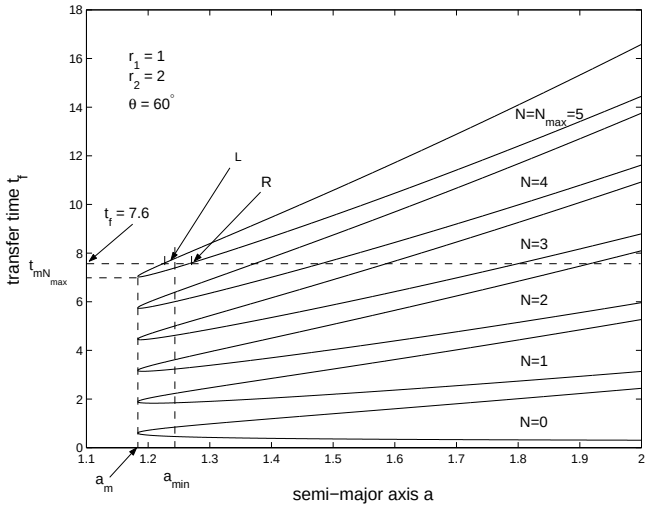

Fig. 6 Subcase 3(a).

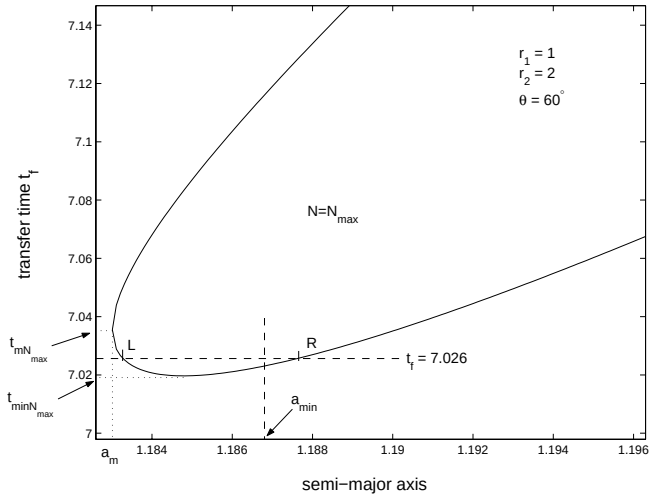

Fig. 7 Subcase 3(b).

We have shown that given a fixed-time fixed-endpoint transfer problem, where the transfer time t_f is given, there are totally $2N_{\max}+1$ solutions; i.e., there are $2N_{\max}+1$ semimajor axes corresponding to one time of flight t_f on t_f versus a plots such as Fig. 2. Each of these $2N_{\max}+1$ semimajor axes corresponds to a transfer orbit. The minimum cost transfer orbit can be obtained by applying the observations we have made in the previous section about the auxiliary transfer problem to these $2N_{\max}+1$ semimajor axes. To do so, we need to first determine where $a_{\min}$ is located on the t_f vs. a plots. This is quite straightforward. Having obtained $a_{\min}$, we can calculate $t_{N\ell}$ and t_{Ns}, the times to transfer from P_1 to P_2 along the two transfer orbits with semimajor axis $a_{\min}$ with N revolutions, where $N = 0, 1, \cdots, N_{\max}$. The subscript '$\ell$' stands for the long path and 's' the short path. Figure 5 shows, for example, t_{Ns} and $t_{N\ell}$ for $N = 4$. Once the location of $a_{\min}$ is determined, there are four cases to consider.

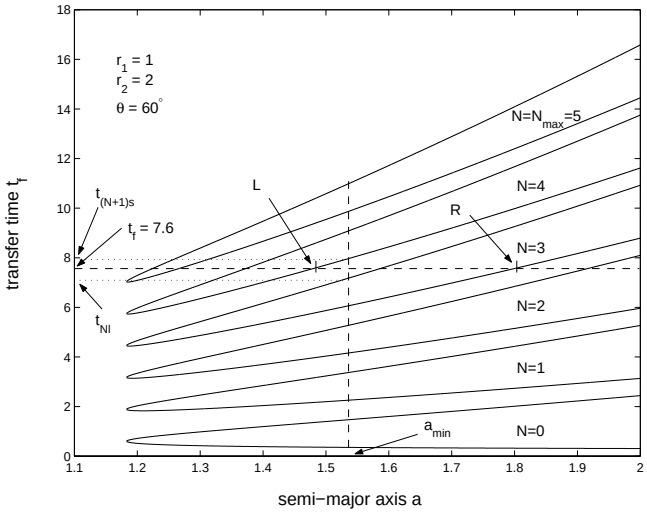

Fig. 8 Case 4.

Case 1. If $N_{\max} = 0$, no revolution is allowed. Apparently there is only one solution in this case, either the long path or the short path solution.

For Case 2, 3, and 4, we assume that $N_{\max} \geq 1$.

Case 2. If $t_{Ns} \leq t_f \leq t_{N\ell}$ and $N \neq N_{\max}$, then $a_{\min}$ is between the semimajor axes of the long path transfer orbit and the short path transfer orbit with $N < N_{\max}$ revolutions, as seen in Fig. 5. Since any long path transfer orbit with semimajor axis less than $a_{\min}$ requires more cost than short path transfer orbits with semimajor axes less than $a_{\min}$, and the closest semimajor axis greater than $a_{\min}$ corresponds to a short path transfer orbit, either the short path N-revolution solution (point R in Fig. 5) or the short path $(N+1)$-revolution solution (point L in Fig. 5) is the minimum cost solution. However, there is no a priori knowledge whether the former or the latter is the minimum cost solution. Thus both transfer orbits corresponding to points R and L need to be calculated, and the one with the smaller cost is the minimum cost transfer orbit. A special subcase occurs when $N = 0$. In this case, the short path 1-revolution solution is the minimum cost solution because there is no short path solution without allowing revolutions.

Case 3. The case when $t_{Ns} \leq t_f \leq t_{N\ell}$ and $N = N_{\max}$

is a little more complicated by the fact that the short path branch for $N \geq 1$ is not monotonically increasing. Instead, t_f has a stationary point. The value of the time of travel at the stationary point is denoted by $t_{\min N}$, as labelled in Fig. 7. Therefore, there are two subcases to consider. The subcase 3(a) where $t_f \geq t_{mN_{\max}}$ is shown in Fig. 6. Following a similar argument as in Case 2, two solutions need to be calculated, which are the long path and the short path solutions corresponding to $N = N_{\max}$ (points L and R in Fig. 6). The smaller of the two renders the minimum cost transfer orbit. On the other hand, the subcase 3(b) where $t_{\min N_{\max}} \leq t_f \leq t_{mN_{\max}}$ is shown in Fig. 7. The two short path $N_{\max}$-revolution solutions (points L and R in Fig. 7) need to be calculated and compared. The smaller one renders the minimum cost transfer orbit.

Case 4. As seen in Fig. 8, in this case $t_{N\ell} \leq t_f \leq t_{(N+1)s}$, then $a_{\min}$ is between the semimajor axes of the N-revolution long path transfer orbit and the $(N+1)$-revolution short path transfer orbit. The $(N+1)$-revolution short path transfer orbit requires less cost than any other solution with semimajor axis less than $a_{\min}$. Similarly, the N-revolution short path transfer orbit requires less cost than any other short path transfer orbit with semimajor axis greater than a_{min}. In addition, any long path transfer orbit requires more cost than the $(N+1)$-revolution short path transfer orbit. Therefore, again, only two solutions need to be calculated and compared. They are the N-revolution and $N+1$ revolution short path solutions (points L and R in Fig. 8). The one with the smaller ΔV represents the minimum cost transfer orbit. Two special subcases occur frequently which correspond to $N = 0$ and $N = N_{\max}$. If $N = 0$, then the 1-revolution short path transfer orbit renders the minimum cost because there is no short path solution without allowing revolutions. On the other hand, if $N = N_{\max}$, two solutions need to be calculated and compared. They are the long path and short path $N_{\max}$-revolution transfer orbits. The one with the smaller ΔV is the minimum cost transfer orbit.

Although these rules that allow one to determine the minimum ΔV solution are illustrated by the plots in Figs. 5-8 for a particular case where $r_2 = 2r_1$ and $\theta = 60^\circ$, these rules apply for all cases as long as the central angle $\theta \leq 180^\circ$. However, similar rules can be obtained easily for the case where the central angle $\theta \geq 180^\circ$. In such cases, the lower branch corresponds to long path transfer orbits and the upper branch corresponds to short path transfer orbits. For the sake of brevity we do not elaborate any further on the latter case; the interested reader should be able to derive the corresponding results vis-à-vis the case $\theta \leq 180^\circ$.

Minimum ΔV, Fixed-Time Two-Impulse Rendezvous Between Circular Orbits

So far, we have presented a procedure for obtaining the fixed-time minimum ΔV transfer orbit between two fixed points on two coplanar unidirectional circular orbits. In this section, we apply this procedure to a slightly different orbital transfer problem encountered frequently in practice. To this end, consider two space vehicles (denoted by I and II) in two coplanar circular orbits moving in the same direction. I is in the lower orbit, and II is in the higher orbit. The initial separation angle θ_0 of I and II is given. The objective is to find the two-impulse minimum ΔV trajectory for I to rendezvous with II in a given fixed time t_f. For the sake of presentation, we will call this *the fixed-time chasing problem*. Essentially, these two problems, the fixed-time fixed-endpoint transfer problem and the fixed-time chasing problem, are related by the fact that the central angle θ defined in the Lambert problem (or in the fixed-endpoint transfer problem) can be written in terms of the initial separation angle θ_0 as

$$\theta = \theta_0 + t_f \omega_2 \tag{5}$$

where ω_2 is the orbital frequency of the outer circular orbit. Once θ is obtained, the minimum cost fixed-time chasing problem becomes a minimum cost fixed-time fixed-point transfer problem, and thus it can be solved using the aforementioned procedure.

For any two circular orbits, minimum cost transfer orbits can be obtained with respect to a range of initial separation angles and transfer times. Thus, a contour plot of the minimum ΔV can be obtained with respect to the separation angles and the transfer times. Figure 9 shows such a contour plot where $r_1 = r_2$, and Fig. 10 shows a contour where $r_1 = 1$ and $r_2 = 1.5$.

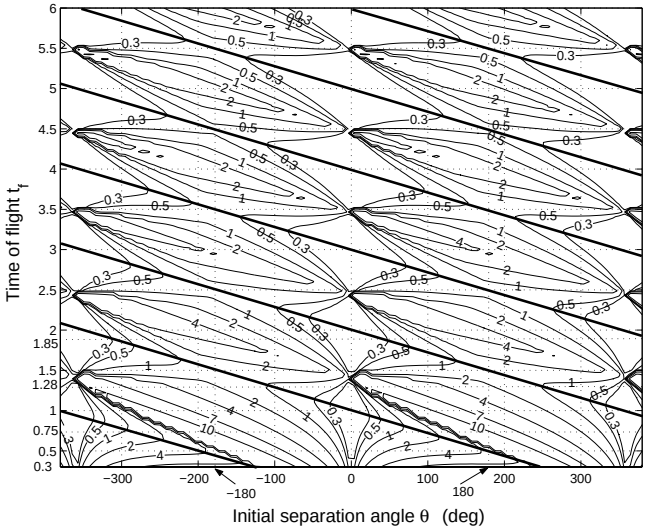

Fig. 9 Contour of ΔV when $r_1 = r_2$.

For the case $r_1 = r_2$ (Fig. 9), the absolute minimum cost (which equals to zero) occurs along the vertical lines $\theta_0 = n \times 360^\circ$, $n = 0, \pm 1, \pm 2, \cdots$. There are isolated non-zero local stationary points which appear in a saddle pattern. Some rather abrupt changes of the costs as t_f or θ_0 changes are observed at points where $t_f \approx n + 0.5$, $n = 1, 2, \cdots$, and θ_0 is slightly larger than integral multiples of 360°. How-

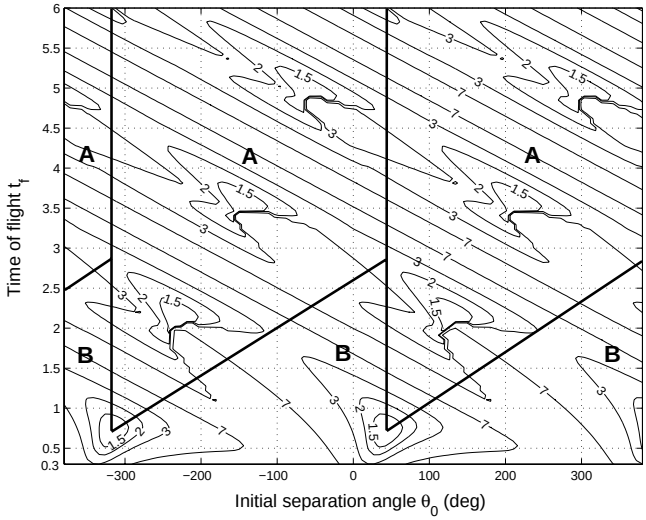

Fig. 10 Contour of ΔV when $r_1 = 1$, $r_2 = 1.5$

ever, when r_2 deviates from r_1, the characteristics of the contours change drastically, as shown in Fig. 10. There are no connected regions of absolute minima, but instead, isolated local minima are observed which resemble a central node pattern. These local minima are indeed global minima provided that $r_2 < 11.94 r_1$ (see Ref. 19) because they correspond to the cost of the Hohmann transfer. As in the case where $r_1 = r_2$, saddle pattern stationary points are also observed, as well as abrupt changes in the cost close to the Hohmann transfers.

Given any fixed-time chasing problem with a combination of t_f and θ_0, the minimum cost can be chosen by referring to the contour plots. It should be noted that the so-obtained solution does not involve any initial and final coasting arcs, i.e., it is the best that can be achieved when the impulses are applied at the initial and final times. However, in many cases, allowing initial and/or terminal coastings helps the two spacecraft obtain a more favorable central angle. As a result, it is possible to perform the desired rendezvous with a lower cost by allowing initial and/or terminal coastings.

Initial and Final Coastings

Suppose that we are given an initial separation angle θ_{00} and a total transfer time t_{f0}, then after an initial coasting period t_{c0} the separation angle θ_0 becomes

$$\begin{aligned}\theta_0 &= \theta_{00} - t_{0c}(\omega_1 - \omega_2) \\ &= \theta_{00} - (t_{f0} - t_{f1})(\omega_1 - \omega_2) \\ &= (\omega_1 - \omega_2)t_{f1} + [\theta_{00} - t_{f0}(\omega_1 - \omega_2)]\end{aligned} \tag{6}$$

hence

$$t_{f1} = \frac{1}{\omega_1 - \omega_2}\theta_0 - \left(\frac{\theta_{00}}{\omega_1 - \omega_2} - t_{f0}\right) \tag{7}$$

where t_{f1} is the transfer time after the initial coasting and ω_1 is the orbital frequency of the inner orbit. Therefore, on the contour plot of θ_0 vs. t_f an initial coasting causes the point (θ_0, t_f) to move down along a straight line with slope of $1/(\omega_1 - \omega_2)$. On the other hand, a final coasting period t_{fc} does not change the initial separation angle, but it shortens the time spent on the transfer orbit; i.e., $t_f = t_{f1} - t_{fc}$. Thus a final coasting causes the point (θ_0, t_f) to move down along a vertical line with θ_0 unchanged.

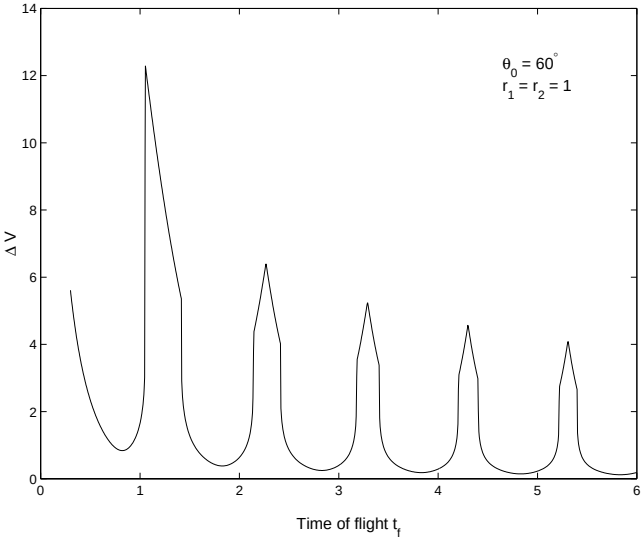

Fig. 11 ΔV vs. t_f when $r_1 = r_2$ and $\theta_0 = 60^\circ$, without coasting.

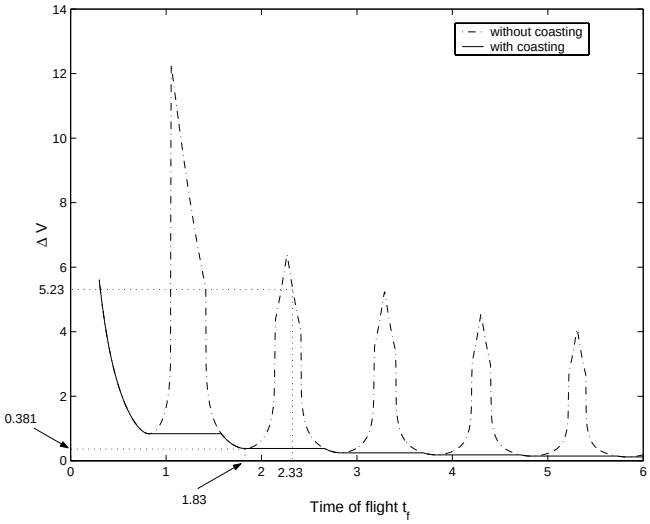

Fig. 12 ΔV vs. t_f when $r_1 = r_2$ and $\theta_0 = 60^\circ$, with terminal coasting.

With these contour plots and the knowledge how initial and terminal coastings affect the solutions, it is straightforward to find the global minimum cost. Given an initial separation angle θ_0 and a transfer time t_f, the initial and terminal coastings can be easily determined by a sliding rule. To make this point clear, let us first refer to Fig. 9 where $r_1 = r_2$. In this case, an initial coasting does not change the relative geometry of the two spacecraft, so only the terminal coasting time needs to be determined. The given θ_0

and t_f correspond to a single point on the contour plot, and any point with the same θ_0 but a transfer time $t_t \le t_f$ also performs the required rendezvous with a terminal coasting of $t_f - t_t$. The transfer time t_t which yields the least ΔV can be easily picked from the contour plot. It is observed that along a vertical line in Fig. 9 as t_f increases, local minima and local maxima of ΔV appear alternately. This is shown in Fig. 11 for the special case when $\theta_0 = 60^\circ$. Interestingly, it can be seen that the values of the local minima decrease as t_f increases, and this trend persists for all $0^\circ \le \theta_0 \le 360^\circ$. Therefore, the optimal amount of terminal coasting can be picked as follows. Given t_f, we decrease t_f while holding θ_0 unchanged until the first local stationary minimum is encountered. Denote the corresponding time t_t. If $\Delta V(\theta_0, t_f) < \Delta V(\theta_0, t_t)$, then no terminal coasting is necessary. If $\Delta V(\theta_0, t_f) > \Delta V(\theta_0, t_t)$, then the terminal coasting is $t_f - t_t$. Figure 12 shows the scheme of obtaining the proper amount of terminal coasting for the case $\theta_0 = 60^\circ$. The dash-dotted line represents the cost without terminal coast which is the same as shown in Fig. 11. The solid line represents the cost with proper terminal coasting. For example, as shown in Fig. 12, for a given time of flight of 2.33, the cost for the rendezvous maneuver without terminal coasting is 5.23. However, this rendezvous can be achieved by a transfer with time of flight of 1.83 plus a terminal coasting of duration 0.5, and the new cost is down to 0.381.

For the case when $r_1 \neq r_2$, we may refer to Fig. 10. The local minima in a center node pattern represent Hohmann transfers. The two solid vertical lines represent transfer problems that can be achieved by a Hohmann transfer by adding an appropriate amount of final coasting. The slanted lines represent transfer problems that can be achieved by a Hohmann transfer by adding an appropriate amount of initial coasting. The whole contour plot is thus divided into upper and lower portions, with the upper portion labeled A, and the lower portion B. It is easy to see that a transfer problem defined in portion A can be achieved by a Hohmann transfer, by adding certain amount of initial and final coastings. On the other hand, portion B consists of transfer problems that cannot be achieved by a Hohmann transfer. However, for some points in portion B, a better cost can be achieved by adding either an initial coasting or a final coasting, and for all others in portion B, no coasting can decrease the cost.

Application Examples

In this section, we make some observations on fixed-time chasing problems arising from servicing satellites in a circular constellation. We are mainly interested in a scenario where there are n satellites distributed (perhaps non-uniformly) along a circular orbit, as shown in Fig. 13. In this figure five satellites are shown, which are labeled I, II, III, IV, and V. The separation angles between satellite I and satellites II, III, IV and V are θ_2, θ_3, θ_4, and θ_5, respectively.

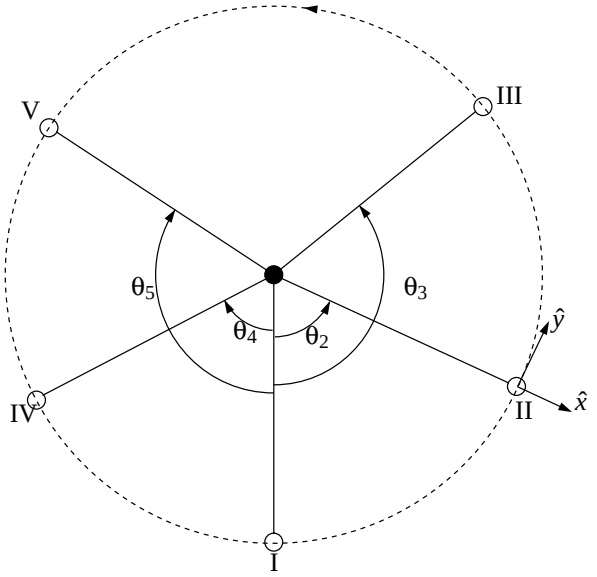

Fig. 13 A satellite constellation on a circular orbit.

Rendezvous with two neighboring satellites

The first question we want to answer is the following: given a fixed total time t_f, find the best rendezvous option for satellite I, namely rendezvous with satellite II (chasing), or rendezvous with satellite IV ("waiting"). An intuitive answer to this question leads one to conjecture that the costs for both options are the same, at least if the corresponding separation angles are the same, i.e., if $\theta_2 = \theta_4$. Indeed, this conclusion can be drawn by a linear analysis using the Clohessy-Wiltshire equations. To demonstrate this analysis, let us consider the current circular orbit as the reference orbit with satellite II being the origin of the associated Euler-Hill coordinate frame for the C-W equations. Let the x axis point along the radial direction, and the y axis point along the velocity direction; see Fig. 13. Then the initial coordinates for the satellite I are given by $(0, -\theta_2)$, and the coordinates for the satellite II are always $(0, 0)$. By using the state transition matrix,[19] the final states and the initial states are related as

$$\begin{bmatrix} 0 \\ 0 \\ \dot{x}_f^- \\ \dot{y}_f^- \end{bmatrix} = \begin{bmatrix} 4-3\cos\tau & 0 & \sin\tau & 2(1-\cos\tau) \\ 6(\sin\tau-\tau) & 1 & -2(1-\cos\tau) & 4\sin\tau-3\tau \\ 3\sin\tau & 0 & \cos\tau & 2\sin\tau \\ 6(\cos\tau-1) & 0 & -2\sin\tau & 4\cos\tau-3 \end{bmatrix} \begin{bmatrix} 0 \\ -\theta_2 \\ \dot{x}_0^+ \\ \dot{y}_0^+ \end{bmatrix} \tag{8}$$

where $(\dot{x}_0^+, \dot{y}_0^+)$ is the velocity vector of I immediately after it leaves its original location, $(\dot{x}_f^-, \dot{y}_f^-)$ is the velocity vector of I immediately before it arrives at the satellite II, and τ is 2π times the transfer time. From the first two rows,

$$\begin{bmatrix} 0 \\ 0 \end{bmatrix} = \begin{bmatrix} 0 \\ -\theta_2 \end{bmatrix} + \begin{bmatrix} \sin\tau & 2(1-\cos\tau) \\ -2(1-\cos\tau) & 4\sin\tau-3\tau \end{bmatrix} \begin{bmatrix} \dot{x}_0^+ \\ \dot{y}_0^+ \end{bmatrix} \tag{9}$$

Equivalently, we have

$$\begin{bmatrix} \dot{x}_0^+ \\ \dot{y}_0^+ \end{bmatrix} = \frac{\theta_2}{8-3\tau\sin\tau-8\cos\tau} \begin{bmatrix} -2(1-\cos\tau) \\ \sin\tau \end{bmatrix} \tag{10}$$

From the last two rows of Eq. (8), we have

$$\begin{bmatrix} \dot{x}_f^- \\ \dot{y}_f^- \end{bmatrix} = \begin{bmatrix} \cos\tau & 2\sin\tau \\ -2\sin\tau & 4\cos\tau - 3 \end{bmatrix} \begin{bmatrix} \dot{x}_0^+ \\ \dot{y}_0^+ \end{bmatrix} \tag{11}$$

Substituting Eq. (10) into Eq. (11), it is easy to show that

$$\begin{bmatrix} \dot{x}_f^- \\ \dot{y}_f^- \end{bmatrix} = \frac{\theta_2}{8 - 3\tau\sin\tau - 8\cos\tau} \begin{bmatrix} 2(1-\cos\tau) \\ \sin\tau \end{bmatrix} = \begin{bmatrix} -\dot{x}_0^+ \\ \dot{y}_0^+ \end{bmatrix} \tag{12}$$

In Euler-Hill coordinate frame, the velocity of I immediately before the first impulse and the velocity of II are zeros. Hence we have that $(\dot{x}_0^+, \dot{y}_0^+)$ and $(-\dot{x}_f^-, -\dot{y}_f^-)$ are the velocity changes (impulses) required for the rendezvous. Thus,

$$\Delta V_0 = \Delta V_f = \left| \begin{bmatrix} \dot{x}_0^+ \\ \dot{y}_0^+ \end{bmatrix} \right| = \frac{\sqrt{5 - 8\cos\tau + 3\cos^2\tau}}{|8 - 3\tau\sin\tau - 8\cos\tau|} |\theta_2| \tag{13}$$

Therefore, the total cost is proportional to the separation angle, which shows that it costs the same for the satellite I to rendezvous with II or IV in a given time as long as the separation angles $\theta_2 = \theta_4$.

Contrary to our intuition and the linear analysis, Fig. 9 from the nonlinear analysis shows no symmetry of the cost about the line $\theta_0 = 0$. In fact, there are many cases where the results deviate from the linear analysis dramatically. For example, consider the case where $\theta_2 = \theta_4 = 100^\circ$ and $t_f = 1$. In this case, the total cost for I to chase II is 10.475, while the total cost for I to chase IV is only 1.869. However, it is not always true that chasing II costs more than chasing IV. For a smaller $t_f = 0.75$ with the same $\theta_2 = \theta_4 = 100^\circ$, it is found that the cost for I to chase II is 1.881, but the cost for I to chase IV is 4.041.

Initial and Terminal Coastings

The observation above was made without allowing any initial or terminal coastings. We have shown that only terminal coasting periods may help decrease the cost for the underlying problem. Let us denote by $f(\tau)$ the coefficient of $|\theta_2|$ in Eq. (13), i.e.,

$$f(\tau) = \frac{\sqrt{5 - 8\cos\tau + 3\cos^2\tau}}{|8 - 3\tau\sin\tau - 8\cos\tau|} \tag{14}$$

which possesses similar characteristics with ΔV in Fig. 11 as a function of the transfer time τ. Therefore, the optimal terminal coasting can be calculated in the same way as in the nonlinear case. It is clear from Eq. (13) that the optimal duration of the terminal coasting is the same for cases with the same time of flight, regardless of the separation angles.

The analysis using the nonlinear equations suggests nonetheless a different scenario. As seen in Fig. 9, the local minima corresponding to two distinct separation angles appear at different transfer times. In fact, the set of all local minima can be approximated very well by slanted solid lines, as shown in Fig. 9. The slope for the slanted lines is $-1/360^\circ$, and they pass through points where the separation angle is zero and the times of flight are integers. With this information, given the separation angle θ_0 and time of flight t_f, the largest transfer time less than t_f that corresponds to a local minimum is given by

$$t_t = n - \frac{\theta_0}{360^\circ} \tag{15}$$

where $n = \lfloor (t_f + \theta_0/360^\circ) \rfloor$ denotes the largest integer smaller than $t_f + \theta_0/360^\circ$. There is no terminal coasting if $\Delta V(t_f, \theta_0) \le \Delta V(t_t, \theta_0)$. Otherwise the terminal coasting time is given by $t_f - t_t$.

It is easy to see from Fig. 9 that a terminal coasting period dramatically decreases the rendezvous cost for some cases. Let us revisit the pursuit problem where $t_f = 1$, and $\theta_2 = \theta_4 = 100^\circ$. Without permitting terminal coasting, a rendezvous with II costs 10.475, and a rendezvous with IV costs 1.869. However, with a terminal coasting period of 0.25, the cost of rendezvous with II decreases to only 1.881, very close to 1.869, the cost of rendezvous with IV which cannot be decreased by allowing terminal coasting.

There is still no clear trend about whether a rendezvous with II or a rendezvous IV will cost less. Thus far we have shown that for the case when $\theta_2 = \theta_4 = 100^\circ$ and $t_f = 0.75$ a rendezvous with IV costs more than a rendezvous with II (4.041 vs. 1.881), and none of these two costs can be decreased by allowing terminal coasting. If $t_f = 2$, then without terminal coasting a rendezvous with II costs 3.313 and a rendezvous with IV costs 1.116. For both cases, the cost can be decreased by adding certain amount of terminal coasting periods: 0.36 for the former and 0.72 for the latter. As a result, the cost for a rendezvous with II decreases to 0.684, less than the cost for a rendezvous with IV, which decreases to 0.914. However, if the total time of travel t_f is 3.5, then without terminal coasting, a rendezvous with II costs 0.625 and a rendezvous with IV costs 0.694. Both cases are in favor of terminal coasting. A terminal coasting of duration 0.78 decreases the cost to rendezvous with II to 0.428, more than the cost to rendezvous with IV which is 0.358 with terminal coasting of duration 0.21. These results are summarized in Table 1.

Table 1 Comparison between the costs of satellite I in rendezvous with satellites II and IV.

t_f	coasting not allowed		coasting allowed			
	Rendezvous II	Rendezvous IV	Rendezvous II		Rendezvous IV	
			coasting time	cost	coasting time	cost
1.0	10.475	1.869	0.25	1.881	N/A	1.869
0.75	1.881	4.041	N/A	1.881	N/A	4.041
2.0	3.313	1.116	0.36	0.684	0.72	0.914
3.5	0.625	0.694	0.78	0.428	0.21	0.358

Rendezvous with two preceding satellites

We now turn our attention to a new question, also arising from the scenario depicted in Fig. 13. The question is to determine the best rendezvous scenario for I: Does a rendezvous with II or a rendezvous with III require a smaller ΔV, given the same transfer time? Henceforth we

assume that $\theta_3 \leq 180^\circ$. An intuitive answer would be to rendezvous with II, because rendezvous with III costs more since III is farther away from I than II is. This is again consistent with Eq. (13) from the linear analysis. However, as is shown next, this intuition based on the linear analysis is not always correct. To see this, let us consider the case where $t_f = 1.85$. It is clear from Fig. 9 that the cost monotonically increases with the initial separation angle in the interval $\theta_0 \in [0, 180^\circ]$. That is, for this particular t_f, it costs more for I to rendezvous with III than to rendezvous with II. However, for the case where $t_f = 1.28$, the cost monotonically increases with θ_0 in the interval $\theta_0 \in [0, 19.192^\circ]$, and decreases monotonically in the interval $[19.192^\circ, 180^\circ]$. That is, when $\theta_2 \geq 19.192^\circ$ and $t_f = 1.28$, the cost for I to rendezvous with III is always less than the cost for I to rendezvous with II.

The observations we have just made do not consider any terminal coasting. With terminal coasting permitted, it is seen that in most cases ($t_f < 1$, e.g.) for the same time of travel, the larger the separation angle is, the larger the cost is. However, it is not hard to find cases where rendezvous with a farther satellite costs less than that with a closer one. For example, let's consider the case where $t_f = 1.42$. For separation angles $\theta_0 < 115^\circ$, we can see that the cost monotonically increases with θ_0, with terminal coasting permitted. However, when $\theta_0 > 115^\circ$, the cost monotonically decreases with θ_0, with terminal coasting permitted (although terminal coasting here does not help decrease the cost). This observation is again inconsistent with the results from the linear analysis.

Conclusions

In this paper, we have studied the optimal fixed-time two-impulse rendezvous problem between two spacecraft orbiting along two coplanar circular orbits in the same direction. First, a fixed-time, fixed-endpoint transfer problem concerning the optimal fixed-time two-impulse transfer between two fixed points on circular orbits is solved using the solution of the multiple-revolution Lambert problem. A solution procedure greatly facilitating the calculation is found, which involves the introduction of an auxiliary transfer problem. This is slightly different than the fixed-time fixed-endpoint transfer problem in the sense that the final time is free. The characteristics of the auxiliary problem are thoroughly explored, and are then used to narrow the $2N_{\max}+1$ solution candidates down to at most two for the optimal fixed-time fixed-endpoint transfer problem. Using this solution procedure, the cost of the original rendezvous problem without coasting periods is easily obtained for all cases of different separation angles and times of travel. Thus a contour plot of the cost can be obtained as a function of the separation angle and the transfer time. This contour plot along with a sliding rule helps find optimal initial and terminal coasting periods, and thus yield solutions to the original rendezvous problem. Two problems concerning a satellite constellation on a circular orbit are studied using the contour plot. The first problem studies the comparison between the rendezvous costs of a satellite with a satellite in front of or a satellite behind it in the constellation. It is found that there is no clear pattern of the rendezvous costs, with or without terminal coasting. This is against the linear analysis which suggests that the costs are the same as long as their separation angles as well as the times of flight are the same. The second problem concerns the comparison between the costs of a satellite to rendezvous with two satellites in front of it in the constellation. With terminal coasting permitted, it is found that for a given time of flight, to rendezvous with the farther satellite costs more than the nearer one for most of the cases. However, there are exceptional cases where to rendezvous with the farther satellite costs less. Without terminal coasting, there no clear trend whether to rendezvous with the farther satellite costs less than the nearer one. Both are against the linear analysis.

Acknowledgement: Support for this work has been provided by AFOSR Grant No: F49620-00-1-0374 and NSF Award No: CMS-9996120.

Appendix: Derivation of $d\Delta V/da$

In this appendix, we give the derivation of $d\Delta V/da$ which can be used to determine $a_{\min}$. The expression for ΔV is given in Eqs. (3) and (4). The velocities at P_1 and P_2 on the transfer orbit are given by[18]

$$v_1 = \sqrt{2\left(E + \frac{\mu}{r_1}\right)}, \qquad v_2 = \sqrt{2\left(E + \frac{\mu}{r_2}\right)} \tag{A.1}$$

where $E = -\mu/(2a)$ is the energy of the transfer orbit. The elevation angles ϕ_1 and ϕ_2 are given by

$$\phi_1 = \tan^{-1}\frac{e\sin f_1}{1+e\cos f_1}, \qquad \phi_2 = \tan^{-1}\frac{e\sin f_1}{1+e\cos f_1}$$

where e is the eccentricity of the transfer orbit, and f_1 and f_2 are the true anomalies at P_1 and P_2 on the transfer orbit, which are given in the following equations.

$$e = \left[1 - \frac{4(s-r_1)(s-r_2)}{d^2}\sin^2\left[\frac{\alpha+\beta}{2}\right]\right]^{1/2} \tag{A.2}$$

$$f_1 = \cos^{-1}\left[\frac{1}{e}\left(\frac{p}{r_1}-1\right)\right] = \cos^{-1}\left[\frac{a(1-e^2)-r_1}{er_1}\right] \tag{A.3}$$

$$f_2 = \cos^{-1}\left[\frac{1}{e}\left(\frac{p}{r_2}-1\right)\right] = \cos^{-1}\left[\frac{a(1-e^2)-r_2}{er_2}\right] \tag{A.4}$$

It is easy to verify that ΔV is only a function of a, provided that r_1, r_2, and θ or d are given. Thus the derivative of ΔV with respect to a is given by

$$\frac{d\Delta V}{da} = \frac{d\Delta V_1}{da} + \frac{d\Delta V_2}{da} \tag{A.5}$$

From Eq. (4), we have

$$\frac{d\Delta V_1}{da} = \frac{\partial \Delta V_1}{\partial v_1}\frac{dv_1}{da} + \frac{\partial \Delta V_1}{\partial \phi_1}\frac{d\phi_1}{da}$$

where,

$$\frac{\partial \Delta V_1}{\partial v_1} = \frac{2v_1 - 2v_{1c}\cos\phi_1}{2\sqrt{v_1^2 + v_{1c}^2 - 2v_1 v_{1c}\cos\phi_1}} = \frac{v_1 - v_{1c}\cos\phi_1}{\Delta V_1}$$

$$\frac{dv_1}{da} = \frac{\partial v_1}{\partial E}\frac{dE}{da} = \frac{1}{2}\frac{2}{v_1}\left(-\frac{\mu}{2}\left(-\frac{1}{a^2}\right)\right) = \frac{\mu}{2a^2 v_1}$$

$$\frac{\partial \Delta V_1}{\partial \phi_1} = \frac{2v_1 v_{1c}\sin\phi_1}{2\sqrt{v_1^2 + v_{1c}^2 - 2v_1 v_{1c}\cos\phi_1}} = \frac{v_1 v_{1c}\sin\phi_1}{\Delta V_1}$$

and $d\phi_1/da$ can be obtained as follows.

$$\frac{d\phi_1}{da} = \frac{\partial \phi_1}{\partial f_1}\frac{df_1}{da} + \frac{\partial \phi_1}{\partial e}\frac{de}{da} \tag{A.6}$$

In Eq. (A.6),

$$\frac{\partial \phi_1}{\partial f_1} = \frac{e\cos f_1(1+e\cos f_1) - e\sin f_1(-e\sin f_1)}{\left[1+\left(\frac{e\sin f_1}{1+e\cos f_1}\right)^2\right](1+e\cos f_1)^2}$$

$$= \frac{e\cos f_1 + e^2}{1+2e\cos f_1 + e^2}$$

$$\frac{\partial \phi_1}{\partial e} = \frac{\sin f_1(1+e\cos f_1) - e\sin f_1\cos f_1)}{\left[1+\left(\frac{e\sin f_1}{1+e\cos f_1}\right)^2\right](1+e\cos f_1)^2}$$

$$= \frac{\sin f_1}{1+2e\cos f_1 + e^2}$$

and df_1/da can be obtained from Eq. (A.3) as follows.

$$\frac{df_1}{da} = \frac{\partial f_1}{\partial e}\frac{de}{da} + \frac{\partial f_1}{\partial a}$$

where

$$\frac{\partial f_1}{\partial e} = -\frac{-2ae^2 r_1 - [a(1-e^2) - r_1]r_1}{e^2 r_1^2\sqrt{1-\left[\frac{a(1-e^2)-r_1}{er_1}\right]^2}}$$

$$= \frac{ae^2 + a - r_1}{e\sqrt{(er_1)^2 - [a(1-e^2)-r_1]^2}}$$

$$\frac{\partial f_1}{\partial a} = \frac{e^2 - 1}{\sqrt{(er_1)^2 - [a(1-e^2)-r_1]^2}}$$

and

$$\frac{de}{da} = \frac{\partial e}{\partial(\alpha+\beta)}\frac{d(\alpha+\beta)}{da} \tag{A.7}$$

In Eq. (A.7)

$$\frac{\partial e}{\partial(\alpha+\beta)} = -\frac{(s-r_1)(s-r_2)\sin(\alpha+\beta)}{ed^2}$$

and it is derived in Ref. 15 that

$$\frac{d(\alpha+\beta)}{da} = -\frac{1}{a}\left(\tan\frac{\alpha}{2} + \tan\frac{\beta}{2}\right)$$

The expression for $d\Delta V_2/da$ can be obtained similarly.

References

[1]Gobetz, F. W. and Doll, J. R., "A Survey of Impulsive Trajectories," *AIAA Journal*, Vol. 7, No. 5, 1969, pp. 801–834.

[2]Billik, B. H. and Roth, H. L., "Studies Relative to Rendezvous between Circular Orbits," *Acta Astronautica*, Vol. 13, 1967, pp. 23–36.

[3]Bell, D. J., "Optimal Space Trajectories–A Review of Published Work," *The Aeronautical Journal of the Royal Aeronautical Society*, Vol. 72, 1968, pp. 141–146.

[4]Jezewski, D. J., Brazzel Jr., J. P., Prust, E. E., Brown, B. G., Mulder, T. A., and Wissinger, D. B., "A Survey of Rendezvous Trajectory Planning," *AAS/AIAA Astrodynamics Conference, Durango, CO, August 19-22, 1991*, Univelt, Inc., San Diego, CA, 1991, pp. 1373–1396, AAS paper 91-505.

[5]Lawden, D. F., *Optimal Trajectories for Space Navigation*, Butterworths, London, 1963.

[6]Lion, P. M. and Handelsman, M., "Primer Vector on Fixed-Time Impulsive Trajectories," *AIAA Journal*, Vol. 6, No. 1, 1968, pp. 127–132.

[7]Jezewski, D. J. and Rozendaal, H. L., "An Efficient Method for Calculating Optimal Free-Space N-Impulse Trajectories," *AIAA Journal*, Vol. 6, No. 11, 1968, pp. 2160–2165.

[8]Gross, L. R. and Prussing, J. E., "Optimal Multiple-Impulse Direct Ascent Fixed-Time Rendezvous," *AIAA Journal*, Vol. 12, No. 7, 1974, pp. 885–889.

[9]Prussing, J. E. and Chiu, J. H., "Optimal Multiple-Impulse Time-Fixed Rendezvous Between Circular Orbits," *Journal of Guidance, Control, and Dynamics*, Vol. 9, No. 1, 1986, pp. 17–22.

[10]Sparks, A., "Satellite Formationkeeping Control in the Presence of Gravity Perturbations," *Proceedings of the American Control Conference, Chicago, IL*, IEEE, Piscataway, NJ, June 28-30, 2000, pp. 844–848.

[11]Wang, P. K., Hadaegh, F. Y., and Lau, K., "Synchronized Formation Rotation and Attitude Control of Multiple Free-Flying Spacecraft," *Journal of Guidance, Control, and Dynamics*, Vol. 22, No. 1, 1999, pp. 28–35.

[12]Alfriend, K. T. and Schaub, H., "Dynamics and Control of Spacecraft Formations: Challenges and Some Solutions," *The Richard H. Battin Astrodynamics Symposium, College Station, TX. in Advances in the Astronautical Sciences*, Vol. 106, American Astronautical Society, March 20-21, 2000, pp. 205–223, AAS Paper 00-259.

[13]Hamilton, W., "Automatic Refueling Coupling for On-Orbit Spacecraft Servicing," *AIAA, ASME, SAE, and ASEE, Joint Propulsion Conference and Exhibit, 25th*, July 10-13 1989, Monterey, CA.

[14]Helton, M. R., "Refurbishable Satellites for Low Cost Communications systems," *Space Communication and Broadcasting*, Vol. 6, 1989, pp. 379–385.

[15]Prussing, J. E., "A Class of Optimal Two-Impulse Rendezvous Using Multiple-Revolution Lambert Solutions," *The Richard H. Battin Astrodynamics Symposium, College Station, TX. in Advances in the Astronautical Sciences.*, Vol. 106, American Astronautical Society, March 20-21, 2000, pp. 17–39, AAS paper 00-250.

[16]Battin, R. H., *An Introduction to the Mathematics and Methods of Astrodynamics*, AIAA Education Series, AIAA, Reston, VA, 1999.

[17]Prussing, J. E., "Geometrical Interpretation of the Angles α and β in Lambert's Problem," *Journal of Guidance, Control, and Dynamics*, Vol. 2, No. 5, 1979, pp. 442–443.

[18]Hale, F. J., *Introduction to Space Flight*, Prentice Hall, Englewood Cliffs, NJ., 1994.

[19]Prussing, J. E. and Conway, B. A., *Orbital Mechanics*, Oxford University Press, Oxford, 1993.